HHS Public Access

Author manuscript

Neuron. Author manuscript; available in PMC 2017 December 07.

Published in final edited form as:

Neuron. 2016 December 07; 92(5): 1093–1105. doi:10.1016/j.neuron.2016.10.031.

Inhibitory control in the cortico-basal ganglia-thalamocortical circuit: complex modulation and its interplay with working memory and decision-making

Wei Wei[1] and **Xiao-Jing Wang**[1,2,3,*]

[1]Center for Neural Science, New York University, New York, NY 10003

[2]NYU-ECNU Institute of Brain and Cognitive Science, NYU Shanghai, Shanghai, China

Summary

We developed a circuit model of spiking neurons that includes multiple pathways in the basal ganglia (BG) and is endowed with feedback mechanisms at three levels: cortical microcircuit, corticothalamic loop and cortico-BG-thalamocortical system. We focused on executive control in a stop-signal task, which is known to depend on BG across species. The model reproduces a range of experimental observations, and shows that the newly discovered feedback projection from external globus pallidus to striatum is crucial for inhibitory control. Moreover, stopping process is enhanced by the cortico-subcortical reverberatory dynamics underlying persistent activity, establishing an inter-dependence between working memory and inhibitory control. Surprisingly, the stop signal reaction time (SSRT) can be adjusted by weights of certain connections but is insensitive to other connections in this complex circuit, suggesting novel circuit-based intervention for inhibitory control deficits associated with mental illness. Our model provides a unified framework for inhibitory control, decision-making and working memory.

Introduction

Across mammalian species from rodent to monkey to human, a conserved brain system is the prefrontal cortex-basal ganglia (BG)-thalamic circuit. This cortico-subcortical system plays a critical role in diverse cognitive functions, including perceptual decision making (Ding and Gold, 2012; Forstmann et al., 2010; Grinband et al., 2006), inhibitory control (Aron et al., 2003; Aron et al., 2007b; Aron and Poldrack, 2006; Jahanshahi et al., 2015), and working memory (Floresco et al., 1999; Isseroff et al., 1982; Mills et al., 2012; Parnaudeau et al., 2013; Wang, 2001; Watanabe and Funahashi, 2012). Recent fMRI study revealed an overlapping cortical representation of executive control and working memory

*Correspondence: xjwang@nyu.edu.
[3]Lead Contact

Author Contributions

W.W. and X.-J.W designed the research. W.W. performed the research and analyzed the data. W.W and X.-J.W wrote the paper.

(Harding et al., 2016). It has also been found that degraded executive control function is usually associated with deficits in working memory in schizophrenia (Gregoire et al., 2012; Zandbelt et al., 2011). Intriguingly, in a task that engaged both perceptual decision making and inhibitory control, the two processes were found to be functionally independent of each other (Middlebrooks and Schall, 2014), raising the question whether they could still share a common underlying circuit. Understanding the circuit mechanism for the interplay between these cognitive functions poses a challenge for both experimental and modeling studies.

Inhibitory control, the ability to cancel a response when a planned action becomes inappropriate, constitutes an essential part of executive function (Schall and Godlove, 2012; Stuphorn, 2015; Verbruggen and Logan, 2009). Impaired inhibition function has been found to be implicated in several neurological disorders such as Parkinson's disease (PD) (Gauggel et al., 2004; Mirabella et al., 2012), attention-deficit hyperactivity disorder (Castellanos et al., 2006; McAlonan et al., 2009), schizophrenia (Hughes et al., 2012; Thakkar et al., 2011; Thakkar et al., 2015; Zandbelt et al., 2011), and also normal aging (Andres et al., 2008; Coxon et al., 2012; Hu et al., 2014). The stop signal task, in which a subject is required to suppress a planned action upon the occurrence of an unexpected stop signal, provides a standard paradigm for investigating inhibitory control (Verbruggen and Logan, 2008, 2009). It allows for the estimation of the latency of a covert stop process, i.e., the stop signal reaction time (SSRT), according to the race model (Boucher et al., 2007; Logan and Cowan, 1984; Logan et al., 2014). SSRT measures the effectiveness of inhibitory control (the shorter is SSRT, the better is one's ability to suppress prepotent but inappropriate action), and it has been widely used to assess impaired inhibitory control in psychiatric patients. A recent experiment provides direct neurophysiological evidence for the involvement of the BG in the stop process: a transient surge of neural activity in the subthalamic nucleus (STN) upon a stop signal presentation, and the corresponding increase of activity in the substantia nigra pars reticulate (SNr) in successful stop signal trials, were well within the window of the SSRT (Schmidt et al., 2013). In pro/anti saccade tasks that involve response inhibition, the higher order thalamus also showed strong modulation during response initiation (Tanaka and Kunimatsu, 2011). Meanwhile, higher-order thalamus receives topographic inputs from the SNr (Gulcebi et al., 2012), and forms reciprocal connections with the frontal cortex (Alexander et al., 1986; Haber and Calzavara, 2009; Parent and Hazrati, 1995). How inhibitory control depends on the multiple pathways through the BG and corticothalamic loop is poorly understood. For instance, which connection pathways in this complex circuit determine SSRT remains unknown. Progress in this direction would shed insights into the operation of a core large-scale brain system as well as specific circuit deficits associated with mental illness.

In this work, we developed a physiologically based network model of spiking neurons with feedback mechanisms at three levels: local cortical microcircuit, corticothalamic loop and cortico-BG-thalamocortical system. We found that the SSRT can be effectively modulated by some specific intrinsic BG connections, in particular the newly discovered pathway from the external segment of the globus pallidus (GPe) to the striatum (Abdi et al., 2015; Dodson et al., 2015; Hegeman et al., 2016; Hernandez et al., 2015; Mallet et al., 2012) plays an essential role in cancelling a planned response in midcourse, in support of the recent physiological report (Mallet et al., 2016). The thalamocortical connection exerts a two-level

modulation of SSRT by switching the distributed attractor network between states with or without persistent activity. On the other hand, the corticothalamic feedback connection does not affect SSRT, even though it gives rise to a bimodal distribution of reaction times; and SSRT is independent of task difficulty when both inhibitory control and perceptual decision making are engaged in a task. These results revealed a complex picture of how SSRT is regulated in the cortico-BG-thalamocortical system.

Results

Distributed attractor network model for inhibitory control

The distributed network model we have constructed includes the cortical circuit (Cx), the BG, and the thalamus (Th), which form a closed loop (Figure 1). This closed loop underlies the inhibitory control function in our model, with putative circuit as depicted in Figure 1A. The Cx shows ramping neuronal activity during movement initiation due to both local reverberation in the cortex and the excitatory drive from the thalamus. The Cx-BG-Th-Cx network forms a positive feedback loop (Figure 1B), which is essential for the ramping in the cortical circuit in the model. In our model, a stop signal is presented as an input to the STN in the BG. The STN receives stop-signal related inputs from two sources: directly from the midbrain, e.g., pedunculopontine tegmental nucleus (PPN) that causes a rapid response in STN (Schmidt et al., 2013), and indirectly from medial frontal areas which are related to inhibitory control (see Discussion). We did not explicitly model the frontal circuit involved in inhibitory control in present model; therefore the stop signal received in the STN represents a combination of both sources. After reaching the STN, the stop signal flows through two routes (Figure 1C). One is from the STN directly to the SNr, which provides a rapid suppression of response initiation by increasing the SNr activity to disrupt the disinhibition to the Th. The second route is from the STN to the striatum (Str) through the GPe (Mallet et al., 2016; see Discussion). Through this route, the stop signal can disrupt the ramping activity in the Str and therefore interfere with the disinhibition to the Th; as a result the thalamic drive to the Cx may become insufficient for the initiation of the planned response in a successful stop signal trial. In the model, neural spiking activity is highly irregular; a response may or may not be cancelled by a stop signal probabilistically depending on the stochastic network dynamics in each single trial.

To examine the mechanism of inhibitory control in our model, we simulated a stop signal task with a constant go signal and a constant stop signal, as usually used in the monkey and human experiments. The neuronal activities of each area are shown in Figure 2 for the go trial (black), successful (blue) and failed (non-cancelled; green) stop signal trials, respectively. The raster plots in each area represent spike trains of the population selective to the go stimulus in a go trial (black) and successful stop signal trial (blue). The lower panel of Figure 2A shows a schematic of the go stimulus, and two stop signal delays (SSDs) (blue, 120 ms; green, 170 ms). In the go trial, the ramping activity in the Cx (Figure 2A) leads to an increase of Str activity (Figure 2D) and a decrease of the SNr activity (Figure 2C), which releases the inhibition to the Th (Figure 2F) and further facilitates the ramping activity in the Cx. The stop signal elevates the STN activity (Figure 2E). In a successful stop signal trial (blue), at the time of stop signal onset, the SNr activity is not suppressed too much by the

striatal input yet, and the elevated STN activity can increase the SNr activity. This leads to a decreased Th activity and terminates the ramping in the Cx. The stop signal flowing through STN-to-GPe-to-Str increases the GPe activity (Figure 2B) and then reduces the Str activity, leading to a weakened go process. In a non-cancelled stop signal trial (green), the SNr activity is strongly suppressed by the striatal input at the time of the stop signal arrival. In this case, the elevated STN activity is insufficient to counteract the strong striatal input to the SNr and disrupt the disinhibittion to the Th, and the response is not cancelled.

Successful stopping happens only in a fraction of the trials for a given SSD. In our model the competition between two selective populations in the Cx results in variably ramping slopes of the winner population, which provides main drive for the fluctuating neuronal activity in the Cx and the downstream circuits from trial to trial. In trials with faster cortical ramping, the SNr also decreases faster and is less likely to increase its activity at the occurrence of stop signal due to the stronger inhibitory drive from the Str. The fraction of non-cancelled stop signal trials (normalized by the performance in go trials) gives the non-cancelled probability, which can be used to estimate the SSRT through the integration method (Logan and Cowan, 1984). The idea is that SSRT quantifies the time needed for a stop process to "win the race" over the go process, therefore non-cancelled trials are those with reaction times (RTs) shorter than the sum of SSD and SSRT, see Figure 3A and Supplemental Experimental Procedures for details. This suggests that the large-scale spiking network model of the cortico-BG-thalamocortical system we have introduced is behaviorally consistent with the race model (Boucher et al., 2007; Logan and Cowan, 1984). The non-cancelled probability as a function of the SSD defines the inhibition function, as shown in Figure 3B. The non-cancelled probability increases with the SSD, from completely cancelling at small SSD to totally failing to cancel at large SSD, as reported in numerous experiments (e.g., Hanes and Schall, 1995; Logan and Cowan, 1984). The mean neuronal activities for non-cancelled and cancelled stop signal trials, and the corresponding latency-matched fast and slow go trials were shown in Figure S1. Here latency-matched fast and slow go trials refer to those go trials with RTs shorter and longer than SSD plus SSRT, respectively. Consistent with recent experimental findings (Schmidt et al., 2013), the variable timing of the striatal activity for go trials determines whether the cancellation of response by stop signal is successful or not (panels D and G in Figure S1). Note that despite the similar activities between Cx and Str in our model (Figure S1), the cortical activity itself does not provide such a determinant since it only receives stop-related activity through the BG-to-Th-to-Cx route, while as suggested by both experiments and our modeling study (see next section), the GPe-to-Str route for stop signal transmission is essential for successful stopping.

SSRT depends on specific BG circuit connections

The stop signal in our model is conveyed through the hyperdirect pathway of the BG to the STN. To cancel a response, the activation of the stop signal on the SNr has to counter-balance the direct pathway input to the SNr. We found that the non-cancelled probability increases with direct pathway strength $g_{Str-SNr}$ (Figure 4A, Left), since it is harder for the stop signal to counter-balance the direct pathway input to the SNr and disrupt the disinhibition to the Th when the strength of the direct pathway is stronger. The SSRT

increases with $g_{Str–SNr}$ (Figure 4A, right), indicating a reduction of stopping function with the increase of the direct pathway strength. At neuronal level, the SNr has a lower spontaneous firing rate and decreases faster during response initiation for a larger $g_{Str–SNr}$ (Figure S2, A), increasing the chance that SNr activity drops to a critically-low level by the onset of the stop signal.

We further checked how the back-propagation of the stop signal from the STN to the Str through the GPe might impact inhibitory control. When the strength of the GPe-to-Str connection, $g_{GPe–Str}$, is increased, we found that the non-cancelled probability is reduced (Figure 4B, left) and the SSRT is decreased (Figure 4B, right). On the other hand, in the absence of GPe-to-Str connection, the model failed completely in performing inhibitory control as indicated by the fact that the non-cancelled probabilities are near 1 (black curve in the left panel of Figure 4B, $g_{GPe–Str} = 0$). Note that for fair comparison, we adjusted the background input to the SNr and kept the spontaneous SNr firing rate unchanged for different $g_{GPe–Str}$, to distinguish from the impact of direct pathway strength $g_{Str–SNr}$, which influences the stopping function by modulating the SNr activity. With a stronger $g_{GPe–Str}$, the stop signal back-propagating to the Str can more easily curtail the ramping activity there, which makes the SNr activity decrease slower, thereby facilitating the stopping function (Figure S2, B). This result resonates with the recent experimental finding of an important role in stopping of arkypallidal cells in the GPe that mediate this feedback projection to the striatum (Mallet et al., 2016). The striatal activity therefore provides a determinant for stopping behavior, where the two routes of stop-related activity transmission, from GPe to Str and from SNr to Cx through Th, converge (Schmidt et al., 2013; see also panels D and G in Figure S1). The inhibition functions for different $g_{Str–SNr}$ (Figure S3, A–B) and $g_{GPe–Str}$ (Figure S3, C–D) are aligned with each other when plotting against the z score of the relative finishing time (ZRFT) (Logan and Cowan, 1984).

We have also performed simulations for an extended circuit, in which the Str neurons are segregated into direct (D1-expressing) and indirect (D2-expressing) pathways neurons, and the GPe neurons are segregated into Ark and Pro types of neurons, respectively (Figure 4C). With this extended circuit, we performed simulations on the impact of Ark-to-Str back-projection on inhibitory control, in which we assumed symmetric projection from Ark neurons to D1- and D2-expressing striatal neurons since no such data available yet (Hegeman et al., 2016). We found a similar impact as shown in Figure 4B (Figure 4D). Therefore, segregation of the Str and GPe into sub-populations does not change the results we have obtained from the simplified circuit. We also showed that choosing a different level of decision threshold at the Cx (Figure S4, A–E) or scaling the sparse GPe-STN connections to all-to-all connections (Figure S4, F–G) does not change the results.

Self-sustained persistent activity facilitates stopping function

When excitatory feedback connections are sufficiently strong, a recurrent neural circuit can generate self-sustained persistent activity (attractor states) (Wang, 2001). The existence of an attractor state in our model is determined by both the local recurrent strength w^+ in the Cx and the feedback strength of the cortico-subcortical loop, for instance, $g_{Th–Cx}$ (see a schematic of the closed Cx-BG-Th loop in Figure 5A, upper panel). We assessed self-

sustained activity states of the model system (in the absence of external input) as a function of w^+ and $g_{Th–Cx}$ (Figure 5A, lower panel). In the left corner, the spontaneous state (SS) is the only stable state, and the neuronal activity of the selective population decays back to the SS after the stimulus is offset. The upper right corner represents a bistable region, where both the SS and the elevated state are stable. When $g_{Th–Cx}$ increases further for a given w^+ (region not shown), the SS becomes unstable and both stimulus-selective (for L and R) populations can be found in that state. Note that the bistable region exists only when w^+ is larger than some critical value, such that the competition between the two (L and R) populations in the Cx is strong enough to implement the winner-take-all mechanism (Wang, 2002). In Figure 5B, we showed the neuronal activity of the winner population in the Cx for two representative samples in the state space (blue and green squares in Figure 5A, lower panel; $w^+ = 1.7$) with $g_{Th–Cx} = 0.26$ nS (blue) and 0.32 nS (green), respectively. When a transient stimulus is shown for 500 ms (Figure 5B, lower panel), it triggers persistent activity for $g_{Th–Cx} = 0.32$ nS (green curve), but not for $g_{Th–Cx} = 0.26$ nS (blue curve). Therefore, by increasing the feedback strength of the big loop, the circuit can be switched from a state without persistent activity to a state that supports self-sustained persistent activity and therefore working memory, under the assumption that local reverberation in the cortex is insufficient to maintain persistent activity. We further note that when $g_{Th–Cx}$ is above some critical value (~0.2 nS here for $w^+ = 1.7$), the Cx shows ramping neuronal activity during the presentation of the stimulus even though only the SS is stable after the stimulus offset. A local circuit with ramping activity but without persistent activity has been investigated in Wong and Wang (2006).

We compared inhibitory control function for these two cases. When there is self-sustained persistent activity, the inhibition function is left-shifted (Figure 5C), indicating a faster go process due to the stronger Cx-BG-Th-Cx feedback loop, as compared to the case when there is no persistent activity. Meanwhile, the SSRT is significantly reduced when there is persistent activity (Figure 5D, colored points), indicating also a faster stop process. This suggests an enhancement of stopping function due to self-sustained persistent activity. To further elucidate the relation between persistent activity dynamics and SSRT, we increased $g_{Th–Cx}$ gradually from the regime without persistent activity to the regime supporting persistent activity with a fixed w^+ ($w^+ = 1.7$). We observed a two-level profile for the SSRT: when $g_{Th–Cx}$ is varied but without crossing the phase boundary (vertical dashed line in Figure 5D), the SSRT is insensitive to this change. There are two different levels of the SSRT, corresponding to the states with and without persistent activity, respectively, when the thalamocortical projection strength is modulated. Note that adjusting $g_{Th–Cx}$ modulates not only the positive feedback strength to the cortical circuit, but also the strength of stop-related activity transmitting to the cortex. In Figure S5 (A–C), we showed that the same conclusion holds when there is a corticothalamic sub-loop. When the corticothalamic projection is not very strong (here $g_{Cx–Th} = 0.2$ nS), the boundary between the regions “Stable SS” and “Bistable” is left-shifted, but the structure of the state space remains qualitatively the same as for the case without corticothalamic projection (Figure S5, A, lower panel). For the two points indicated in the state space, the cortical activity shows persistent activity for one, but not for the other when receiving a transient stimulus (Figure S5, B). We found that the two-

level modulation of SSRT by the thalamocortical connection strength still holds when there exists a corticothalamic sub-loop (Figure S5, C).

It is interesting to check further how the SSRT depends on w^+. From panel D in Figure S5, we found that the SSRT decreases monotonically with the increase of w^+, i.e., the stopping function is enhanced with stronger locally reverberatory dynamics. This differential modulation of the SSRT by g_{Th-Cx} and w^+ results from the fact that in addition to provide positive feedback to the Cx, the thalamocortical connection, but not the recurrent connection within the Cx, also transmits the stop-related activity that terminates ramping activity and motor response.

Functional independence of perceptual decision and inhibitory control

Our model provides a framework to explore the interaction between inhibitory control and perceptual decision making when both processes are engaged in a task. To study this, we introduced a stop signal in the random-dot motion discrimination task, in which both stimulus-selective populations receive inputs, with the relative strength of the inputs encoding the motion coherence c' (Wang, 2002; Wong and Wang, 2006). When there is no stop signal, the model performances and mean RTs as a function of c' are shown in Figure 6A–B. For non-cancelled stop signal trials, the performances and mean RTs show similar trends as those for go trials (Figure S6). In stop signal trials, the non-cancelled probability increases with c', therefore decreases with the task difficulty (Figure 6C). However, the SSRT is insensitive to c' (Figure 6D; one way ANOVA, $p = 0.59$). This suggests that the task difficulty, which strongly influences the perceptual decision process (Figure 6A–B), has no impact on the stop process. This can also be seen from Figure 6E, which shows that the mean neuronal activities of cancelled (successful) stop signal trials are almost indistinguishable for low and high coherences. It therefore indicates the functional independence between the choosing and stopping processes, consistent with a recent behavioral experiment (Middlebrooks and Schall, 2014). Figure S7 shows that the inhibition functions are aligned with each other for different c' when plotted against the ZRFT.

Note that we have made no assumptions about how the stop signal is presented or how the response is executed. Our model therefore suggests that the functional independence between choosing and stopping processes generalizes across modalities of the stop signal and response. This can be tested, for instance, by performing motion discrimination task with auditory stop signal and/or key press response.

Impact of corticothalamic sub-loop on stopping function

Up to this point, we have not included the corticothalamic connection in the model (except in Figure S5, A–C), so we can examine the cortico-BG-thalamocortical loop. Now we investigate the impact of such a connection on stopping function by including nonzero corticothalamic connection strength, g_{Cx-Th}. This sub-loop makes it possible for the reverberatory dynamics to rebound in spite of transient suppression by a stop signal, leading to slow responses and a bimodal distribution of RTs in non-cancelled trials (Figure 7A, lower panel; $g_{Cx-Th} = 0.4$ nS). Note that the second peak has totally different origin from the first one. While the first peak is driven by stimulus and reflects the most likely time for

ramping cortical activity crossing the threshold, the second peak is driven mainly by noise when the constant stop signal enhances SNr activity and diminishes cortical ramping activity. This is reflected by the very steep rising of Cx activity for trials with RTs located near the second peak. The RT distributions for different SSDs are shown in Figure S8 (A–B) with $g_{Cx–Th}$ = 0.4 nS. Interestingly, this computational finding is supported by empirical observations from experiments using rats (Schmidt et al., 2013). Our model thus suggests that the bimodal RT distribution for rats performing a stop signal task might result from a strong corticothalamic sub-loop. Note that our model assumes that even when the sensory stimulus for signaling stop is transient, the internal representation of the stop signal is sustained. This assumption is crucial and remains to be tested in future experiments.

Figure 7A (upper panel) shows the cdf of RTs. The classical integration method for estimating SSRT is not longer applicable, since there is a substantial fraction of non-cancelled stop signal trials (with long RTs) for which there are no latency-matched go trials. We therefore estimated the SSRT using a modified integration method (Mayse et al., 2014), where the divergent point of the cdf for non-cancelled stop signal trials and go trials was used to estimate the SSRT (see Supplemental Experimental Procedures for details).

We then investigated how the strength of the Cx-Th sub-loop influences the SSRT. Figure 7C (upper panel) shows a schematic of the circuit. We increased $g_{Cx–Th}$ from 0 to 0.6 nS and estimated the SSRT for each value of $g_{Cx–Th}$ with $g_{Th–Cx}$ = 0.26 nS, for which there is no persistent activity in the network (Figure 7C, middle panel) when receiving a transient stimulus (Figure 7C, lower panel). As shown in Figure 7C, the SSRT is independent of $g_{Cx–Th}$ (one way ANOVA, p = 0.74). Note that the same conclusion also holds when there is persistent activity in the circuit. In Figure S8 (panel C), the Cx circuit shows persistent activity with $g_{Th–Cx}$ = 0.32 nS (upper panel) when receiving a transient stimulus (lower panel). We found that the SSRT is independent of $g_{Cx–Th}$ (Figure S8, D; one way ANOVA, p = 0.60).

Discussion

Inhibitory control of action is a central for flexible behavior, characterized by SSRT which has been used to quantify inhibitory control ability as well its impairment in psychiatric illness. The BG are known to play an important role in inhibitory control, but only recent work has begun to dissect its underlying circuit mechanism in the BG. The spiking neural circuit model presented in this paper accounts for salient experimental observations including the bimodal distribution of RTs in a stop signal task (Schmidt et al., 2013), as well as the surprising finding that SSRT is independent of task difficulty in perceptual decision making (Middlebrooks and Schall, 2014). This biologically constrained model with explanatory power revealed a complex picture of how different connection pathways modulate SSRT. This is an important new insight into the BG function, opening up new experiments to test the model and ideas about potential circuit-specific ways to remedy inhibitory control deficits in psychiatric patients. Another conceptual advance is to establish an inter-dependence between inhibitory control ability and working memory in the cortico-BG-thalamocortical system.

In this work, we propose a distributed attractor network model for executive control. A stop signal enters the BG through the hyperdirect pathway, and then interacts with the direct and indirect pathways to subserve inhibitory control in stop-signal tasks. This cortico-BG-thalamocortical system involves three feedback loops at multiple levels, and a main finding of this work is complex dependence of the effectiveness of inhibitory control on various pathways as summarized in Figure 8. The SSRT is increased when the "go" process becomes more potent by increasing the Str-to-SNr strength. On the other hand, the SSRT is decreased when the GPe-to-Str connection is stronger, which permits more potent backpropagation of the stop signal to the Str. The SSRT is also decreased when the network is switched from a state without persistent activity to a state supporting persistent activity, establishing a link between working memory and inhibitory control. Our model offers explanation for several recent experimental observations in stop signal tasks. First, the GPe-to-Str feedback connection mediated by arkypallidal cells is essential for inhibitory control (Mallet et al. 2016). Second, when inhibitory control is combined with perceptual decision making, SSRT is independent of the task difficulty (Middlebrooks and Schall, 2014). Third, our model suggests that a non-negligible corticothalamic sub-loop leads to a bimodal distribution of RTs for non-cancelled stop signal trials (Schmidt et al., 2013), and predicts that the strength of corticothalamic projection does not change SSRT. This model prediction can be tested in future experiments.

Previously, closed cortico-BG-thalamocortical loop has been proposed to implement different cognitive functions. This loop has been suggested to implement working memory retrieval and response selection (Schroll et al., 2012; Vitay and Hamker, 2010). In another modeling study, imbalanced direct and hyperdirect pathways led to the lost of action selection and the generation of oscillatory activity (Leblois et al., 2006). Recently, the competition between hyperdirect and indirect pathways has been investigated using a nested diffusion model to differentiate the stopping and no-go processes (Dunovan et al., 2015). Wiecki and Frank (2013) proposed a Cx-BG-Th-Cx loop model including several frontal cortical areas that implemented different response inhibition tasks. None of these studies, however, have investigated how the effectiveness of inhibitory control, quantified by SSRT, depends on various connection pathways. In this work we build a distributed attractor network model instantiated by the Cx-BG-Th-Cx closed loop, such that the local recurrent connection within the cortical circuit is by itself not enough to maintain persistent activity. It is conceivable that persistent activity can be generated intrinsically within certain local areas (like the prefrontal cortex in monkey), but depends on the thalamocortical loop in other areas (such as the premotor/motor system in rodents; Svoboda lab, personal communication). Our model provides a general framework for inhibitory control, perceptual decision making and working memory, and allows for investigating how the SSRT depends on connection and dynamic properties of the network.

The role of the BG in action control was commonly hypothesized to exert through disinhibition to downstream structures (Hikosaka et al., 2000; but see Turner and Desmurget, 2010 for an alternative view), although disinhibition may be context-dependent (Goldberg et al., 2013). Interruption of the disinhibition mechanism of the BG lied in the core of our model for inhibitory control, and has been supported by recent experiments (Schmidt et al., 2013). The indirect pathway of the BG has important roles in proactive inhibitory control

(Majid et al., 2013) and perceptual decision making (Wei et al., 2015). Here we showed that modulation of the relative weights of the BG pathways could effectively modulate the SSRT, which provides a possible source for individual difference of the SSRT. Recently, goal directed or habitual behavior in rodents was associated with latency changes for the activation of direct and indirect pathways striatal neurons (O'Hare et al., 2016). It has been found that in goal directed response the indirect pathway striatal neurons showed a shorter latency than the direct pathway neurons. The difference between the latencies is about 20 ms, which is much shorter than the time for evidence accumulation and the SSD, therefore unlikely to impact the process we investigated. The GPe has been found to be also involved in anti-saccade task (Yoshida and Tanaka, 2016). Recent experiments have identified two distinct classes of GPe neurons, with one class forming reciprocal connections with the striatum (Ark type) and the other forming reciprocal connections with the STN (Pro type) (Dodson et al., 2015; Mallet et al., 2012). The input sources to stop-related activity of Arky GPe neurons are not clarified yet, with transmission of stop-related activity from slowly activated STN neurons to the GPe as a possible source (Mallet et al., 2016). In this work we assumed a constant input to the STN representing the stop signal, which is a combination of rapid input directly from the midbrain (e.g., PPN) and slower input indirectly from the medial frontal areas, and that the stop signal received by the GPe is transmitted from the STN. Since how the two GPe classes interact with each other during behavioral tasks is not experimentally characterized yet, we consider one single class of GPe neurons that project both to the STN and the striatum. Under this simplification, the GPe activity increases and the striatal activity decreases with the occurrence of stop signal, consistent with recent experiments (Mallet et al., 2016). Similarly, we also simplified the two classes of striatal neurons expressing D1 and D2 receptors, respectively, to a homogeneous class due to the non-distinction of them in existing experiments (Ding and Gold, 2010; Schmidt et al., 2013). We have shown that taking into account of the subclasses of striatal and GPe neurons do not qualitatively change results obtained from the simplified circuit assuming homogeneous populations in these nuclei. Further experimental data about interaction between the two types of striatal and GPe neurons will help future models to reveal the functional roles of these segregation under normal and pathological states. Moreover, since our model is biophysically realistic with spiking neurons and synaptic dynamics, it can be used, in a separate study, to explore different dynamical operating regimes (such as spike-to-spike synchrony or population rhythms) and their impact on inhibitory control function, as well as differential contributions of various (such as AMPA versus NMDA) receptor types to executive control, bridging levels from molecules to circuit dynamics to behavior.

Another direction in future extensions of our model is to elucidate differential contributions of several frontal areas to inhibitory control, including the right inferior frontal cortex (rIFC) and pre-supplementary motor area (preSMA) (Aron, 2011; Jha et al., 2015; Swann et al., 2012), whose roles in stopping are still controversial. The rIFC might directly participate in inhibitory control process by projecting to the BG (Aron et al., 2007a; Aron et al., 2014; Swann et al., 2009), or be important for detection of the stop signal (Duann et al., 2009; Hampshire et al., 2010; Sharp et al., 2010). The preSMA is more related to rule-based, motivational or contextual modulation (Isoda and Hikosaka, 2007; Jha et al., 2015; Ridderinkhof et al., 2004; Scangos and Stuphorn, 2010). These two frontal areas could

interact with the BG by projecting to the STN (Aron et al., 2007a; Cavanagh et al., 2011; Isoda and Hikosaka, 2008), representing a frontal source of stop-related signal flowing to the BG whose strength correlates with efficacy in stopping for normal subjects (Forstmann et al., 2012) and deficits in inhibitory control during aging (Coxon et al., 2012). They can also selectively activate the indirect pathway striatal neurons (Ghahremani et al., 2012; Jahfari et al., 2011). Fixation neurons in the frontal eye field (FEF) have been found to show activity that resembles with the stop process (Boucher et al., 2007; Hanes et al., 1998). A local network mechanism for inhibitory control through fixation neurons in the FEF accompanied by a top-down control signal has been proposed (Lo et al., 2009). Primary motor cortex also displayed neuronal activity related to action inhibition (Stinear et al., 2009), where fixation-like neurons were observed recently (Zagha et al., 2015). Other subcortical areas, such as the superior colliculus (SC) (Pare and Hanes, 2003) and basal forebrain (Mayse et al., 2015) have also been found to be involved in inhibitory control. Whether these areas play a causal role or they are downstream of a core inhibitory control circuit remains to be better understood in the future. Ultimately, a large-scale brain circuit model is needed in order to systematically investigate multiple input sources for any given brain region and how interconnections between many cortical and subcortical structures actually work.

Both the thalamocortical and corticostriatal dysfunctions have been related to cognitive deficits in mental disorders (Anticevic et al., 2014; Gregoire et al., 2012; Parnaudeau et al., 2013; Zandbelt et al., 2011). Our model predicts that adjusting thalamocortical strength leads to a two-level modulation of the SSRT, which could be tested experimentally by selectively optogenetic inactivation of neurons in corresponding thalamic nuclei (Paz et al., 2013). Adjusting the corticostriatal strength, on the contrary, will lead to a gradual modulation of the SSRT, since that does not change the maximal drive from the thalamus to the cortex and influence the existence of persistent activity. Impact of corticostriatal projection on inhibitory control could exert through its efficacy in modulating decision threshold level (Lo and Wang, 2006): a degraded corticostriatal projection will lead to a higher decision threshold, which then increases the SSRT (Figure S4, A–E). The distinct impact on the SSRT induced by adjusting thalamocortical and corticostriatal connections, i.e., two-level versus gradual modulation, could be a differential signature for the involvement of these two loci. Inasmuch as distinct pathways may be impaired in different psychiatric patient groups (e.g. schizophrenia versus obsessive-compulsive disorder), the identification of specific connections that mostly effectively modulate SSRT could suggest better loci of “circuit-based” treatment for improving inhibitory control.

In conclusion, our distributed attractor network model offers a unified framework for investigating inhibitory control, perceptual decision making and working memory. This model provides experimental testable predictions about interaction among these functions. It can also be applied to the study of neurological diseases such as PD and schizophrenia, and shed further insights about deficits in the executive functions from a distributed attractor network point of view.

Experimental Procedures

Behavioral task simulation

We considered a classical paradigm for inhibitory control, the stop signal task. Both the stimulus and the stop signal are constant. We simulated a two-alternative choice task and considered two types of stimulus. The first kind is a go stimulus indicating the position of the target (left or right) for the response as used in the classical stop signal task (Boucher et al., 2007; Logan and Cowan, 1984). The second one is a random-dots stimulus as used in the motion discrimination task (Newsome et al., 1989; Roitman and Shadlen, 2002). A correct go trial or failed (non-cancelled) stop signal trial is defined as a trial in which the firing rate of the selective population in the Cx crosses a threshold at 15 Hz. A successful stop signal trial is defined as a trial in which the firing rate of the selective population in the Cx never crosses the threshold. Note that the results in the paper do not depend on the choice of threshold value in the Cx (Figure S4, A–E). When there is no stop signal, model performance is defined as the fraction of correct go trials. In stop signal trials, the non-cancelled probability is defined as the ratio between the fraction of non-cancelled stop signal trials and the performance when there is no stop signal. This definition ensures that the non-cancelled probability approaches to 1 for large SSD.

Network modeling

The full circuit includes three brain areas: the cortical network (Cx), the BG, and the thalamus (Th). The Cx is the same as described in previous work (Wang, 2002), but with a lower background input to support distributed attractor state. The present model extends an earlier one (Wei et al., 2015) by including the thalamus and replacing the effect of SC in that model by a constant threshold in the Cx. We used the leaky integrate-and-fire model for all the neurons.

For full details on the experimental procedures, please refer to the Supplemental Experimental Procedures.

Supplementary Material

Refer to Web version on PubMed Central for supplementary material.

Acknowledgments

This work was supported by a Swartz Foundation Fellowship (W.W.), the National Institutes of Health Grant R01 MH062349 and the Naval Research Grant N00014-13-1-0297 (X.-J.W.). We thank J. Rubin for insightful discussion, and F. Song and J. Murray for comments and carefully reading an early version of the manuscript.

References

Abdi A, Mallet N, Mohamed FY, Sharott A, Dodson PD, Nakamura KC, Suri S, Avery SV, Larvin JT, Garas FN, et al. Prototypic and arkypallidal neurons in the dopamine-intact external globus pallidus. J Neurosci. 2015; 35:6667–6688. [PubMed: 25926446]

Alexander GE, DeLong MR, Strick PL. Parallel organization of functionally segregated circuits linking basal ganglia and cortex. Annu Rev Neurosci. 1986; 9:357–381. [PubMed: 3085570]

Andres P, Guerrini C, Phillips LH, Perfect TJ. Differential effects of aging on executive and automatic inhibition. Dev Neuropsychol. 2008; 33:101–123. [PubMed: 18443972]

Anticevic A, Cole MW, Repovs G, Murray JD, Brumbaugh MS, Winkler AM, Savic A, Krystal JH, Pearlson GD, Glahn DC. Characterizing thalamo-cortical disturbances in schizophrenia and bipolar illness. Cereb Cortex. 2014; 24:3116–3130. [PubMed: 23825317]

Aron A, Schlaghecken F, Fletcher P, Bullmore ET, Eimer M, Barker R, Sahakian B, Robbins T. Inhibition of subliminally primed responses is mediated by the caudate and thalamus: evidence from functional MRI and Huntington's disease. Brain. 2003; 126:713–723. [PubMed: 12566291]

Aron AR. From reactive to proactive and selective control: developing a richer model for stopping inappropriate responses. Biol Psychiatry. 2011; 69:e55–68. [PubMed: 20932513]

Aron AR, Behrens TE, Smith S, Frank MJ, Poldrack RA. Triangulating a cognitive control network using diffusion-weighted magnetic resonance imaging (MRI) and functional MRI. J Neurosci. 2007a; 27:3743–3752. [PubMed: 17409238]

Aron AR, Durston S, Eagle DM, Logan GD, Stinear CM, Stuphorn V. Converging evidence for a fronto-basal-ganglia network for inhibitory control of action and cognition. J Neurosci. 2007b; 27:11860–11864. [PubMed: 17978025]

Aron AR, Poldrack RA. Cortical and subcortical contributions to Stop signal response inhibition: role of the subthalamic nucleus. J Neurosci. 2006; 26:2424–2433. [PubMed: 16510720]

Aron AR, Robbins TW, Poldrack RA. Inhibition and the right inferior frontal cortex: one decade on. Trends Cogn Sci. 2014; 18:177–185. [PubMed: 24440116]

Boucher L, Palmeri TJ, Logan GD, Schall JD. Inhibitory control in mind and brain: an interactive race model of countermanding saccades. Psychol Rev. 2007; 114:376–397. [PubMed: 17500631]

Castellanos FX, Sonuga-Barke EJ, Milham MP, Tannock R. Characterizing cognition in ADHD: beyond executive dysfunction. Trends Cogn Sci. 2006; 10:117–123. [PubMed: 16460990]

Cavanagh JF, Wiecki TV, Cohen MX, Figueroa CM, Samanta J, Sherman SJ, Frank MJ. Subthalamic nucleus stimulation reverses mediofrontal influence over decision threshold. Nat Neurosci. 2011; 14:1462–1467. [PubMed: 21946325]

Coxon JP, Van Impe A, Wenderoth N, Swinnen SP. Aging and inhibitory control of action: cortico-subthalamic connection strength predicts stopping performance. J Neurosci. 2012; 32:8401–8412. [PubMed: 22699920]

Ding L, Gold JI. Caudate encodes multiple computations for perceptual decisions. J Neurosci. 2010; 30:15747–15759. [PubMed: 21106814]

Ding L, Gold JI. Separate, causal roles of the caudate in saccadic choice and execution in a perceptual decision task. Neuron. 2012; 75:865–874. [PubMed: 22958826]

Dodson PD, Larvin JT, Duffell JM, Garas FN, Doig NM, Kessaris N, Duguid IC, Bogacz R, Butt SJ, Magill PJ. Distinct developmental origins manifest in the specialized encoding of movement by adult neurons of the external globus pallidus. Neuron. 2015; 86:501–513. [PubMed: 25843402]

Duann JR, Ide JS, Luo X, Li CS. Functional connectivity delineates distinct roles of the inferior frontal cortex and presupplementary motor area in stop signal inhibition. J Neurosci. 2009; 29:10171–10179. [PubMed: 19675251]

Dunovan K, Lynch B, Molesworth T, Verstynen T. Competing basal ganglia pathways determine the difference between stopping and deciding not to go. Elife. 2015; 4

Floresco SB, Braaksma DN, Phillips AG. Thalamic-cortical-striatal circuitry subserves working memory during delayed responding on a radial arm maze. J Neurosci. 1999; 19:11061–11071. [PubMed: 10594086]

Forstmann BU, Anwander A, Schafer A, Neumann J, Brown S, Wagenmakers EJ, Bogacz R, Turner R. Cortico-striatal connections predict control over speed and accuracy in perceptual decision making. Proc Natl Acad Sci USA. 2010; 107:15916–15920. [PubMed: 20733082]

Forstmann BU, Keuken MC, Jahfari S, Bazin PL, Neumann J, Schafer A, Anwander A, Turner R. Cortico-subthalamic white matter tract strength predicts interindividual efficacy in stopping a motor response. NeuroImage. 2012; 60:370–375. [PubMed: 22227131]

Gauggel S, Rieger M, Feghoff TA. Inhibition of ongoing responses in patients with Parkinson's disease. J Neurol Neurosurg Psychiatry. 2004; 75:539–544. [PubMed: 15026491]

Ghahremani DG, Lee B, Robertson CL, Tabibnia G, Morgan AT, De Shetler N, Brown AK, Monterosso JR, Aron AR, Mandelkern MA, et al. Striatal Dopamine D-2/D-3 Receptors Mediate Response Inhibition and Related Activity in Frontostriatal Neural Circuitry in Humans. J Neurosci. 2012; 32:7316–7324. [PubMed: 22623677]

Goldberg JH, Farries MA, Fee MS. Basal ganglia output to the thalamus: still a paradox. Trends Neurosci. 2013; 36:695–705. [PubMed: 24188636]

Gregoire S, Rivalan M, Le Moine C, Dellu-Hagedorn F. The synergy of working memory and inhibitory control: behavioral, pharmacological and neural functional evidences. Neurobiol Learn Mem. 2012; 97:202–212. [PubMed: 22197651]

Grinband J, Hirsch J, Ferrera VP. A neural representation of categorization uncertainty in the human brain. Neuron. 2006; 49:757–763. [PubMed: 16504950]

Gulcebi MI, Ketenci S, Linke R, Hacioglu H, Yanali H, Veliskova J, Moshe SL, Onat F, Cavdar S. Topographical connections of the substantia nigra pars reticulata to higher-order thalamic nuclei in the rat. Brain Res Bull. 2012; 87:312–318. [PubMed: 22108631]

Haber SN, Calzavara R. The cortico-basal ganglia integrative network: the role of the thalamus. Brain Res Bull. 2009; 78:69–74. [PubMed: 18950692]

Hampshire A, Chamberlain SR, Monti MM, Duncan J, Owen AM. The role of the right inferior frontal gyrus: inhibition and attentional control. NeuroImage. 2010; 50:1313–1319. [PubMed: 20056157]

Hanes DP, Patterson WF 2nd, Schall JD. Role of frontal eye fields in countermanding saccades: visual, movement, and fixation activity. J Neurophysiol. 1998; 79:817–834. [PubMed: 9463444]

Hanes DP, Schall JD. Countermanding saccades in macaque. Vis Neurosci. 1995; 12:929–937. [PubMed: 8924416]

Harding IH, Harrison BJ, Breakspear M, Pantelis C, Yucel M. Cortical representations of cognitive control and working memory are dependent yet non-Interacting. Cereb Cortex. 2016; 26:557–565. [PubMed: 25249406]

Hegeman DJ, Hong ES, Hernandez VM, Chan CS. The external globus pallidus: progress and perspectives. Eur J Neurosci. 2016; 43:1239–1265. [PubMed: 26841063]

Hernandez VM, Hegeman DJ, Cui Q, Kelver DA, Fiske MP, Glajch KE, Pitt JE, Huang TY, Justice NJ, Chan CS. Parvalbumin+ Neurons and Npas1+ Neurons Are Distinct Neuron Classes in the Mouse External Globus Pallidus. J Neurosci. 2015; 35:11830–11847. [PubMed: 26311767]

Hikosaka O, Takikawa Y, Kawagoe R. Role of the basal ganglia in the control of purposive saccadic eye movements. Physiol Rev. 2000; 80:953–978. [PubMed: 10893428]

Hu S, Chao HH, Zhang S, Ide JS, Li CS. Changes in cerebral morphometry and amplitude of low-frequency fluctuations of BOLD signals during healthy aging: correlation with inhibitory control. Brain Struct Funct. 2014; 219:983–994. [PubMed: 23553547]

Hughes ME, Fulham WR, Johnston PJ, Michie PT. Stop-signal response inhibition in schizophrenia: behavioural, event-related potential and functional neuroimaging data. Biol Psychol. 2012; 89:220–231. [PubMed: 22027085]

Isoda M, Hikosaka O. Switching from automatic to controlled action by monkey medial frontal cortex. Nat Neurosci. 2007; 10:240–248. [PubMed: 17237780]

Isoda M, Hikosaka O. Role for subthalamic nucleus neurons in switching from automatic to controlled eye movement. J Neurosci. 2008; 28:7209–7218. [PubMed: 18614691]

Isseroff A, Rosvold HE, Galkin TW, Goldman-Rakic PS. Spatial memory impairments following damage to the mediodorsal nucleus of the thalamus in rhesus monkeys. Brain Res. 1982; 232:97–113. [PubMed: 7034865]

Jahanshahi M, Obeso I, Rothwell JC, Obeso JA. A fronto-striato-subthalamic-pallidal network for goal-directed and habitual inhibition. Nat Rev Neurosci. 2015; 16:719–732. [PubMed: 26530468]

Jahfari S, Waldorp L, van den Wildenberg WPM, Scholte HS, Ridderinkhof KR, Forstmann BU. Effective Connectivity Reveals Important Roles for Both the Hyperdirect (Fronto-Subthalamic) and the Indirect (Fronto-Striatal-Pallidal) Fronto-Basal Ganglia Pathways during Response Inhibition. J Neurosci. 2011; 31:6891–6899. [PubMed: 21543619]

Jha A, Nachev P, Barnes G, Husain M, Brown P, Litvak V. The frontal control of stopping. Cereb Cortex. 2015; 25:4392–4406. [PubMed: 25754518]

Leblois A, Boraud T, Meissner W, Bergman H, Hansel D. Competition between feedback loops underlies normal and pathological dynamics in the basal ganglia. J Neurosci. 2006; 26:3567–3583. [PubMed: 16571765]

Lo CC, Boucher L, Pare M, Schall JD, Wang XJ. Proactive inhibitory control and attractor dynamics in countermanding action: a spiking neural circuit model. J Neurosci. 2009; 29:9059–9071. [PubMed: 19605643]

Lo CC, Wang XJ. Cortico-basal ganglia circuit mechanism for a decision threshold in reaction time tasks. Nat Neurosci. 2006; 9:956–963. [PubMed: 16767089]

Logan GD, Cowan WB. On the ability to inhibit thought and action: A theory of an act of control. Psychol Rev. 1984; 91:295–327.

Logan GD, Van Zandt T, Verbruggen F, Wagenmakers EJ. On the ability to inhibit thought and action: general and special theories of an act of control. Psychol Rev. 2014; 121:66–95. [PubMed: 24490789]

Majid DA, Cai W, Corey-Bloom J, Aron AR. Proactive selective response suppression is implemented via the basal ganglia. J Neurosci. 2013; 33:13259–13269. [PubMed: 23946385]

Mallet N, Micklem BR, Henny P, Brown MT, Williams C, Bolam JP, Nakamura KC, Magill PJ. Dichotomous organization of the external globus pallidus. Neuron. 2012; 74:1075–1086. [PubMed: 22726837]

Mallet N, Schmidt R, Leventhal D, Chen F, Amer N, Boraud T, Berke JD. Arkypallidal cells send a stop signal to striatum. Neuron. 2016; 89:308–316. [PubMed: 26777273]

Mayse JD, Nelson GM, Avila I, Gallagher M, Lin SC. Basal forebrain neuronal inhibition enables rapid behavioral stopping. Nat Neurosci. 2015; 18:1501–1508. [PubMed: 26368943]

Mayse JD, Nelson GM, Park P, Gallagher M, Lin SC. Proactive and reactive inhibitory control in rats. Front Neurosci. 2014; 8:104. [PubMed: 24847204]

McAlonan GM, Cheung V, Chua SE, Oosterlaan J, Hung SF, Tang CP, Lee CC, Kwong SL, Ho TP, Cheung C, et al. Age-related grey matter volume correlates of response inhibition and shifting in attention-deficit hyperactivity disorder. Br J Psychiatry. 2009; 194:123–129. [PubMed: 19182173]

Middlebrooks PG, Schall JD. Response inhibition during perceptual decision making in humans and macaques. Atten Percept Psychophys. 2014; 76:353–366. [PubMed: 24306985]

Mills KL, Bathula D, Dias TG, Iyer SP, Fenesy MC, Musser ED, Stevens CA, Thurlow BL, Carpenter SD, Nagel BJ, et al. Altered cortico-striatal-thalamic connectivity in relation to spatial working memory capacity in children with ADHD. Front Psychiatry. 2012; 3:2. [PubMed: 22291667]

Mirabella G, Iaconelli S, Romanelli P, Modugno N, Lena F, Manfredi M, Cantore G. Deep brain stimulation of subthalamic nuclei affects arm response inhibition in Parkinson's patients. Cereb Cortex. 2012; 22:1124–1132. [PubMed: 21810782]

Newsome WT, Britten KH, Movshon JA. Neuronal correlates of a perceptual decision. Nature. 1989; 341:52–54. [PubMed: 2770878]

O'Hare JK, Ade KK, Sukharnikova T, Van Hooser SD, Palmeri ML, Yin HH, Calakos N. Pathway-Specific Striatal Substrates for Habitual Behavior. Neuron. 2016; 89:472–479. [PubMed: 26804995]

Pare M, Hanes DP. Controlled movement processing: superior colliculus activity associated with countermanded saccades. J Neurosci. 2003; 23:6480–6489. [PubMed: 12878689]

Parent A, Hazrati LN. Functional anatomy of the basal ganglia. I. The cortico-basal ganglia-thalamo-cortical loop. Brain Res Brain Res Rev. 1995; 20:91–127. [PubMed: 7711769]

Parnaudeau S, O'Neill PK, Bolkan SS, Ward RD, Abbas AI, Roth BL, Balsam PD, Gordon JA, Kellendonk C. Inhibition of mediodorsal thalamus disrupts thalamofrontal connectivity and cognition. Neuron. 2013; 77:1151–1162. [PubMed: 23522049]

Paz JT, Davidson TJ, Frechette ES, Delord B, Parada I, Peng K, Deisseroth K, Huguenard JR. Closed-loop optogenetic control of thalamus as a tool for interrupting seizures after cortical injury. Nat Neurosci. 2013; 16:64–70. [PubMed: 23143518]

Ridderinkhof KR, Ullsperger M, Crone EA, Nieuwenhuis S. The role of the medial frontal cortex in cognitive control. Science. 2004; 306:443–447. [PubMed: 15486290]

Roitman JD, Shadlen MN. Response of neurons in the lateral intraparietal area during a combined visual discrimination reaction time task. J Neurosci. 2002; 22:9475–9489. [PubMed: 12417672]

Scangos KW, Stuphorn V. Medial frontal cortex motivates but does not control movement initiation in the countermanding task. J Neurosci. 2010; 30:1968–1982. [PubMed: 20130204]

Schall JD, Godlove DC. Current advances and pressing problems in studies of stopping. Curr Opin Neurobiol. 2012; 22:1012–1021. [PubMed: 22749788]

Schmidt R, Leventhal DK, Mallet N, Chen F, Berke JD. Canceling actions involves a race between basal ganglia pathways. Nat Neurosci. 2013; 16:1118–1124. [PubMed: 23852117]

Schroll H, Vitay J, Hamker FH. Working memory and response selection: a computational account of interactions among cortico-basalganglio-thalamic loops. Neural Netw. 2012; 26:59–74. [PubMed: 22075035]

Sharp DJ, Bonnelle V, De Boissezon X, Beckmann CF, James SG, Patel MC, Mehta MA. Distinct frontal systems for response inhibition, attentional capture, and error processing. Proc Natl Acad Sci USA. 2010; 107:6106–6111. [PubMed: 20220100]

Stinear CM, Coxon JP, Byblow WD. Primary motor cortex and movement prevention: where Stop meets Go. Neurosci Biobehav Rev. 2009; 33:662–673. [PubMed: 18789963]

Stuphorn V. Neural mechanisms of response inhibition. Curr Opin Behav Sci. 2015; 1:64–71.

Swann N, Tandon N, Canolty R, Ellmore TM, McEvoy LK, Dreyer S, DiSano M, Aron AR. Intracranial EEG reveals a time- and frequency-specific role for the right inferior frontal gyrus and primary motor cortex in stopping initiated responses. J Neurosci. 2009; 29:12675–12685. [PubMed: 19812342]

Swann NC, Cai W, Conner CR, Pieters TA, Claffey MP, George JS, Aron AR, Tandon N. Roles for the pre-supplementary motor area and the right inferior frontal gyrus in stopping action: electrophysiological responses and functional and structural connectivity. NeuroImage. 2012; 59:2860–2870. [PubMed: 21979383]

Tanaka M, Kunimatsu J. Contribution of the central thalamus to the generation of volitional saccades. Eur J Neurosci. 2011; 33:2046–2057. [PubMed: 21645100]

Thakkar KN, Schall JD, Boucher L, Logan GD, Park S. Response inhibition and response monitoring in a saccadic countermanding task in schizophrenia. Biol Psychiatry. 2011; 69:55–62. [PubMed: 20970778]

Thakkar KN, Schall JD, Logan GD, Park S. Cognitive control of gaze in bipolar disorder and schizophrenia. Psychiatry Res. 2015; 225:254–262. [PubMed: 25601802]

Turner RS, Desmurget M. Basal ganglia contributions to motor control: a vigorous tutor. Curr Opin Neurobiol. 2010; 20:704–716. [PubMed: 20850966]

Verbruggen F, Logan GD. Response inhibition in the stop-signal paradigm. Trends Cogn Sci. 2008; 12:418–424. [PubMed: 18799345]

Verbruggen F, Logan GD. Models of response inhibition in the stop-signal and stop-change paradigms. Neurosci Biobehav Rev. 2009; 33:647–661. [PubMed: 18822313]

Vitay J, Hamker FH. A computational model of Basal Ganglia and its role in memory retrieval in rewarded visual memory tasks. Front Comput Neurosci. 2010; 4

Wang XJ. Synaptic reverberation underlying mnemonic persistent activity. Trends Neurosci. 2001; 24:455–463. [PubMed: 11476885]

Wang XJ. Probabilistic decision making by slow reverberation in cortical circuits. Neuron. 2002; 36:955–968. [PubMed: 12467598]

Watanabe Y, Funahashi S. Thalamic mediodorsal nucleus and working memory. Neurosci Biobehav Rev. 2012; 36:134–142. [PubMed: 21605592]

Wei W, Rubin JE, Wang XJ. Role of the indirect pathway of the basal ganglia in perceptual decision making. J Neurosci. 2015; 35:4052–4064. [PubMed: 25740532]

Wiecki TV, Frank MJ. A computational model of inhibitory control in frontal cortex and basal ganglia. Psychol Rev. 2013; 120:329–355. [PubMed: 23586447]

Wong KF, Wang XJ. A recurrent network mechanism of time integration in perceptual decisions. J Neurosci. 2006; 26:1314–1328. [PubMed: 16436619]

Yoshida A, Tanaka M. Two types of neurons in the primate globus pallidus external segment play distinct roles in antisaccade generation. Cereb Cortex. 2016; 26:1187–1199. [PubMed: 25577577]

Zagha E, Ge X, McCormick DA. Competing neural ensembles in motor cortex gate goal-directed motor output. Neuron. 2015; 88:565–577. [PubMed: 26593093]

Zandbelt BB, van Buuren M, Kahn RS, Vink M. Reduced proactive inhibition in schizophrenia is related to corticostriatal dysfunction and poor working memory. Biol Psychiatry. 2011; 70:1151–1158. [PubMed: 21903198]

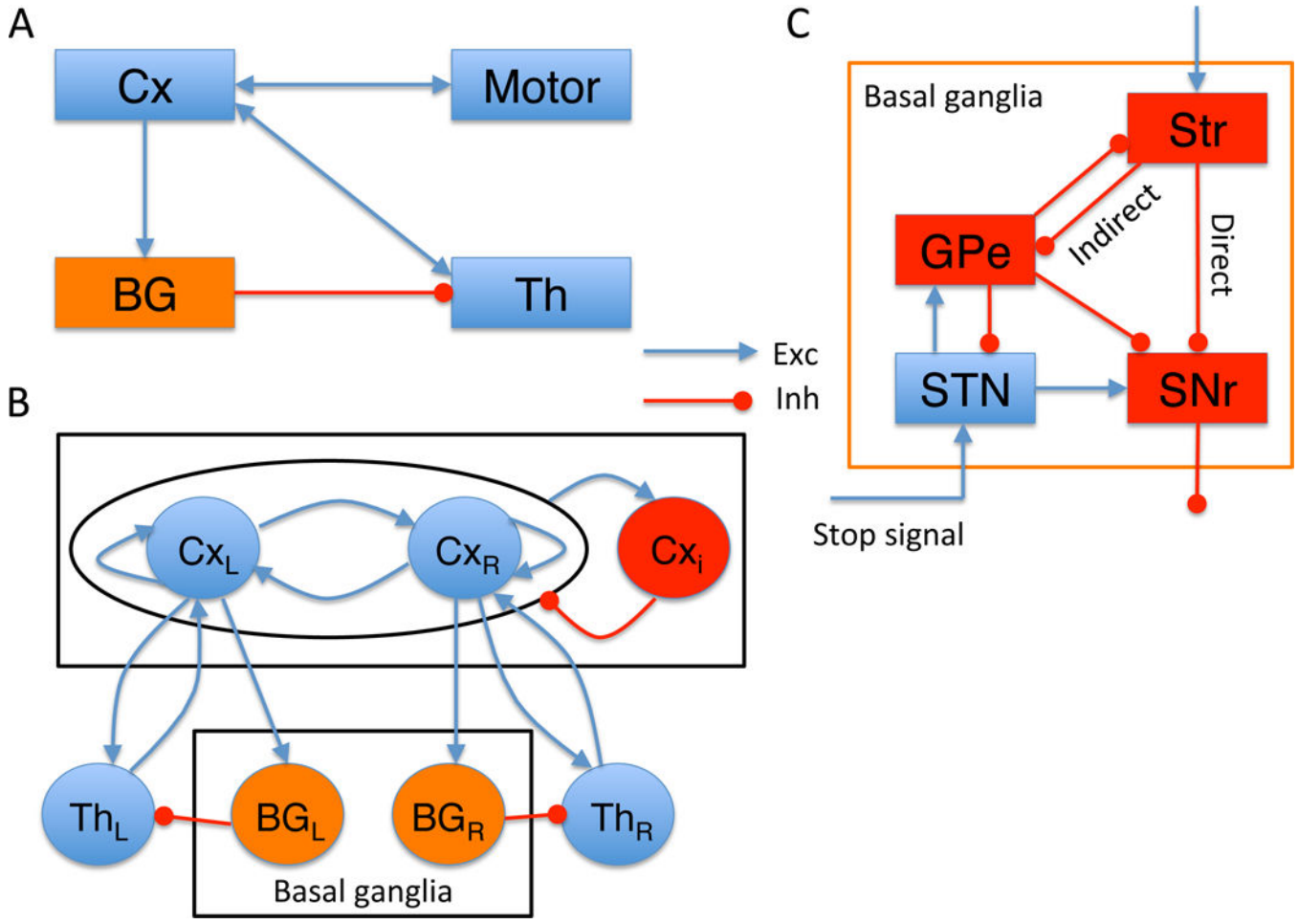

Figure 1. Schematic of the cortico-basal ganglia-thalamocortical loop model

(A) Circuit for Inhibitory control implemented by the Cx-BG-Th loop. (B) The "zoomed in" circuit diagram from (A). In each local area there are two neural populations selective for targets (L=left, R=right). This setting is suitable for simulating a two-alternative choice task. The model is endowed with feedback loops at three levels: local cortical recurrent network, thalamocortical loop, and global cortico-BG-thalamocortical loop. (C) The "zoomed in" BG circuit diagram. The Str projects to the output nucleus (SNr) through two pathways: the direct pathway (denoted as "Direct") from the Str directly to the SNr, and the indirect pathway (denoted as "Indirect") from the Str through the GPe, STN to the SNr. For simplicity, we use SNr to represent both SNr and GPi, the two output nuclei of the BG. The stop signal originates from separate cortical or/and subcortical area and is simplified as a direct input to the STN, entering the BG via the hyperdirect pathway. Note that the projection from the GPe to the Str allows the stop signal to be fed back to the Str. Cx_i represents the inhibitory population in the Cx. Abbreviations: Cx, cortex; BG, basal ganglia; Str, striatum; GPe, external segment of the globus pallidus (GP); GPi, internal segment of the GP; STN, subthalamic nucleus; SNr, substantia nigra pars reticulata; Motor, cortical/subcortical motor area. Exc, excitatory; Inh, inhibitory.

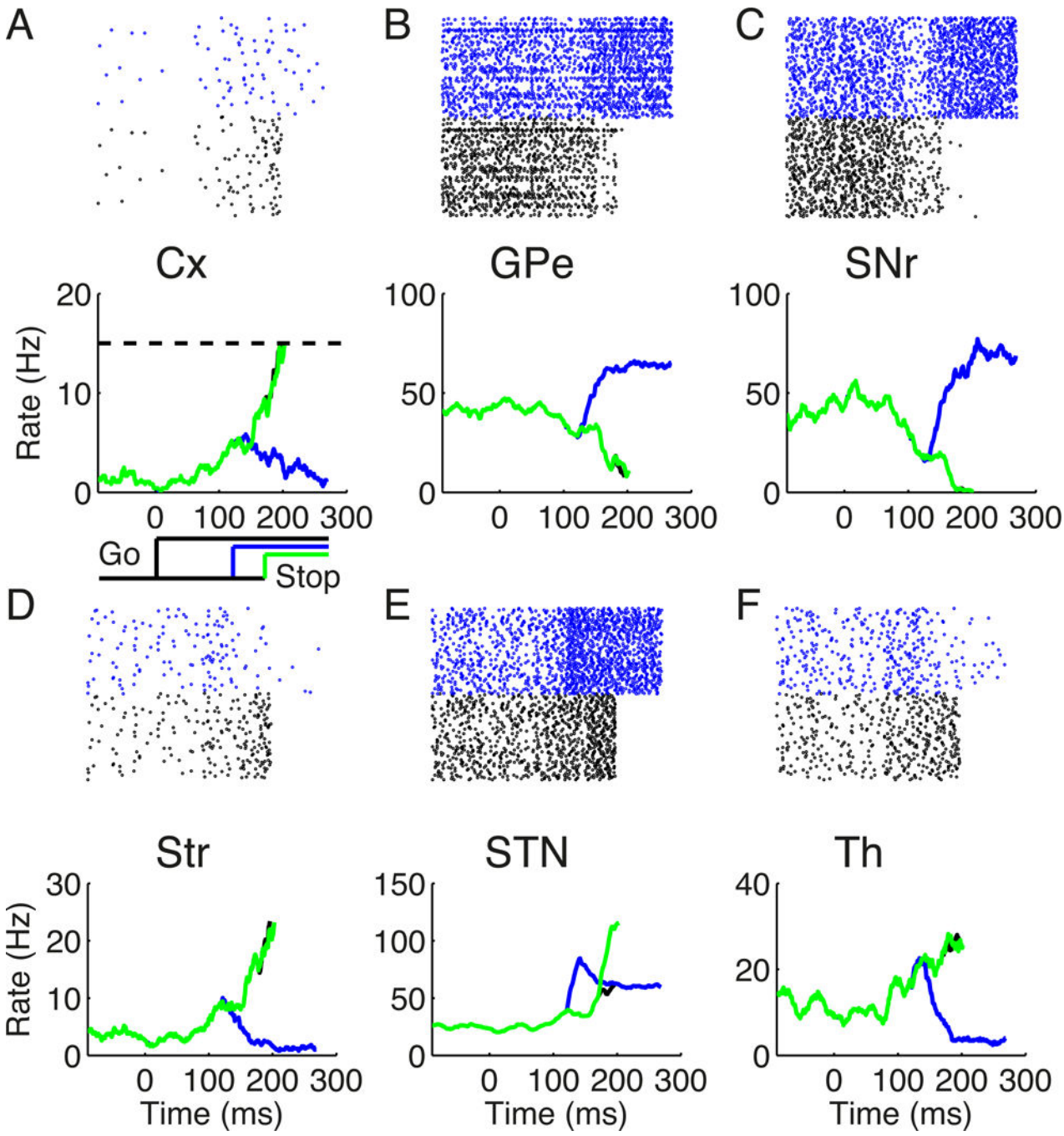

Figure 2. Single-trial simulations of the stop-signal task

Raster plots show the spike trains for a go trial (black) and a successful stop signal trial (blue) in each area (A–F; upper panels). The population firing rates in each area (A–F; lower panels) are shown for a go trial (black), and successful (blue) and failed (green) stop signal trials. The schematic in (A) illustrates a constant go stimulus that is turned on at time 0 (black) and two SSDs for the stop signal at 120 ms (blue) and 170 ms (green), respectively.

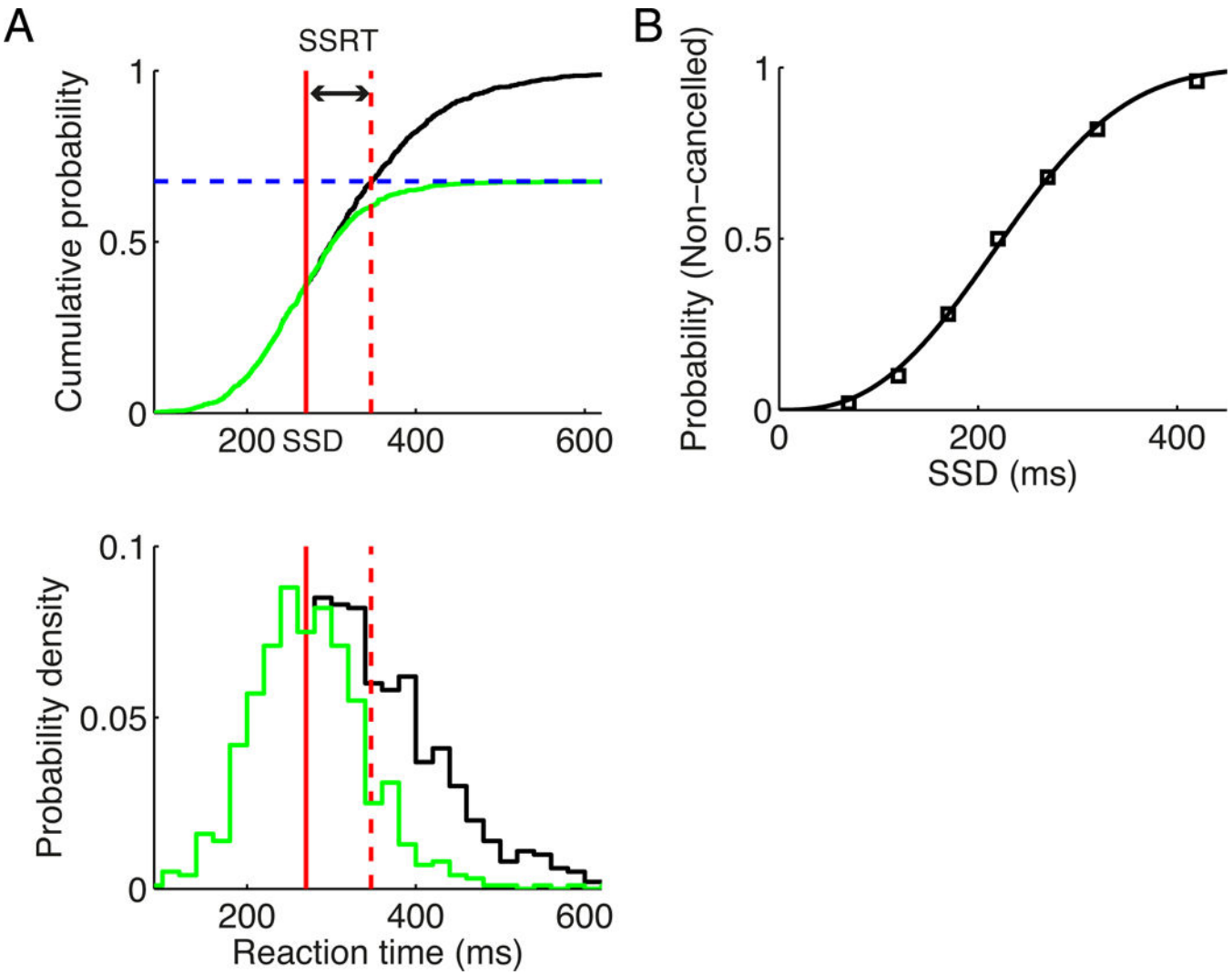

Figure 3. SSRT and inhibition function from the model

(A) Upper panel: integration method for estimating the SSRT. The black curve represents the cumulative density function (cdf) for the reaction times (RTs) of go trials, and green curve represents the cdf for the RTs of non-cancelled stop signal trials with SSD = 270 ms, scaled by the overall non-cancelled probability (fraction of non-cancelled stop signal trials, blue dashed line). The vertical red dashed line represents the intersection time of the blue dashed line and the black curve. The solid red line indicates the SSD. The interval between the vertical solid and dashed red lines gives the SSRT. Lower panel: RT probability densities for the go trials (black curve) and non-cancelled stop signal trials (green curve; scaled by non-cancelled probability). (B) The non-cancelled probability as a function of the SSD (the inhibition function), which is fitted by the Weibull function.

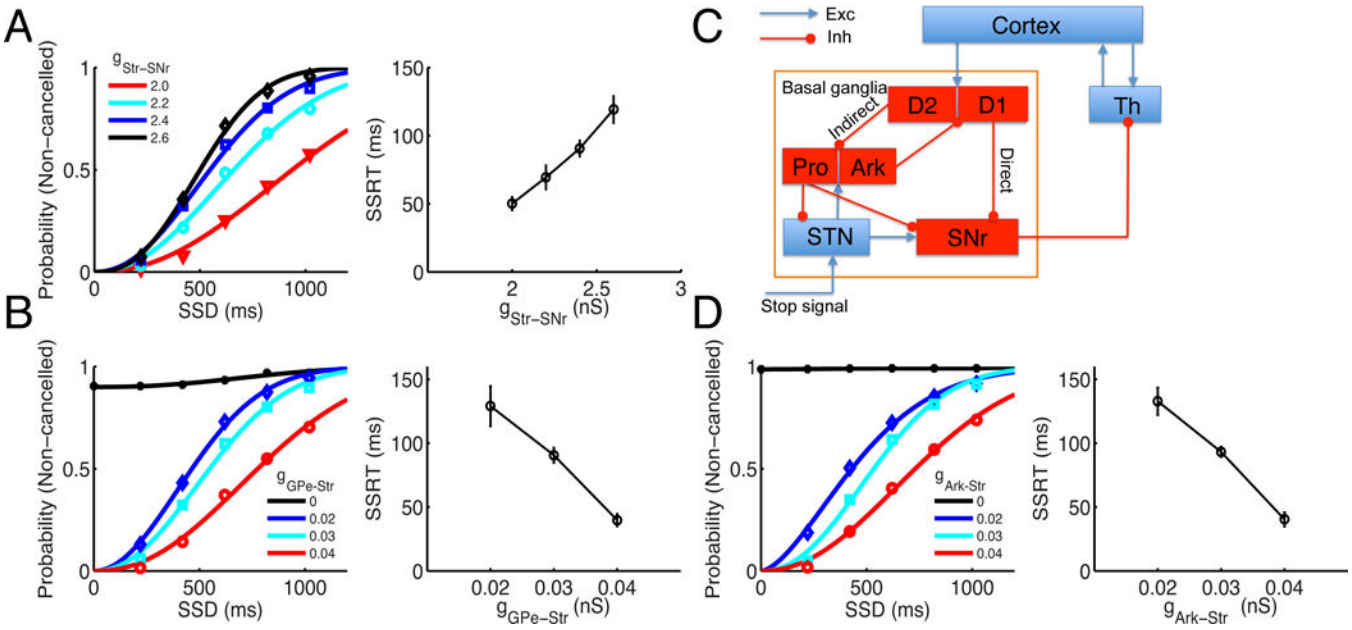

Figure 4. SSRT depends on weights of specific connections in the BG

(A) Left: dependence of inhibition functions on $g_{Str–SNr}$. Right: the SSRT increases with a larger $g_{Str–SNr}$. (B) Left: dependence of inhibition functions on $g_{GPe–Str}$. Right: the SSRT decreases with a larger $g_{GPe–Str}$. (C) Schematic of the extended BG circuit. The Str neurons are segregated into direct (D1-expressing) and indirect (D2-expressing) pathways neurons, and the GPe neurons are segregated into Ark and Pro types of neurons. The Ark neurons project back to both types of Str neurons, and the Pro neurons project to the STN and SNr. The indirect pathway striatal neurons and STN neurons project to both Ark and Pro neurons. (D) Left: dependence of inhibition functions on the back-projection strength from the Ark neurons to the Str, $g_{Ark–Str}$. Right: the SSRT decreases with a larger $g_{Ark–Str}$. Error bars indicate s.d. of SSRT values estimated for each SSD. Note that in (B) and (D), for fair comparison when $g_{GPe–Str}$ or $g_{Ark–Str}$ is varied, the spontaneous firing rate of the SNr is fixed by adjusting the external input rate v_{ext} to it. The inhibition functions in (A), (B), and (D) are fitted by the Weibull function.

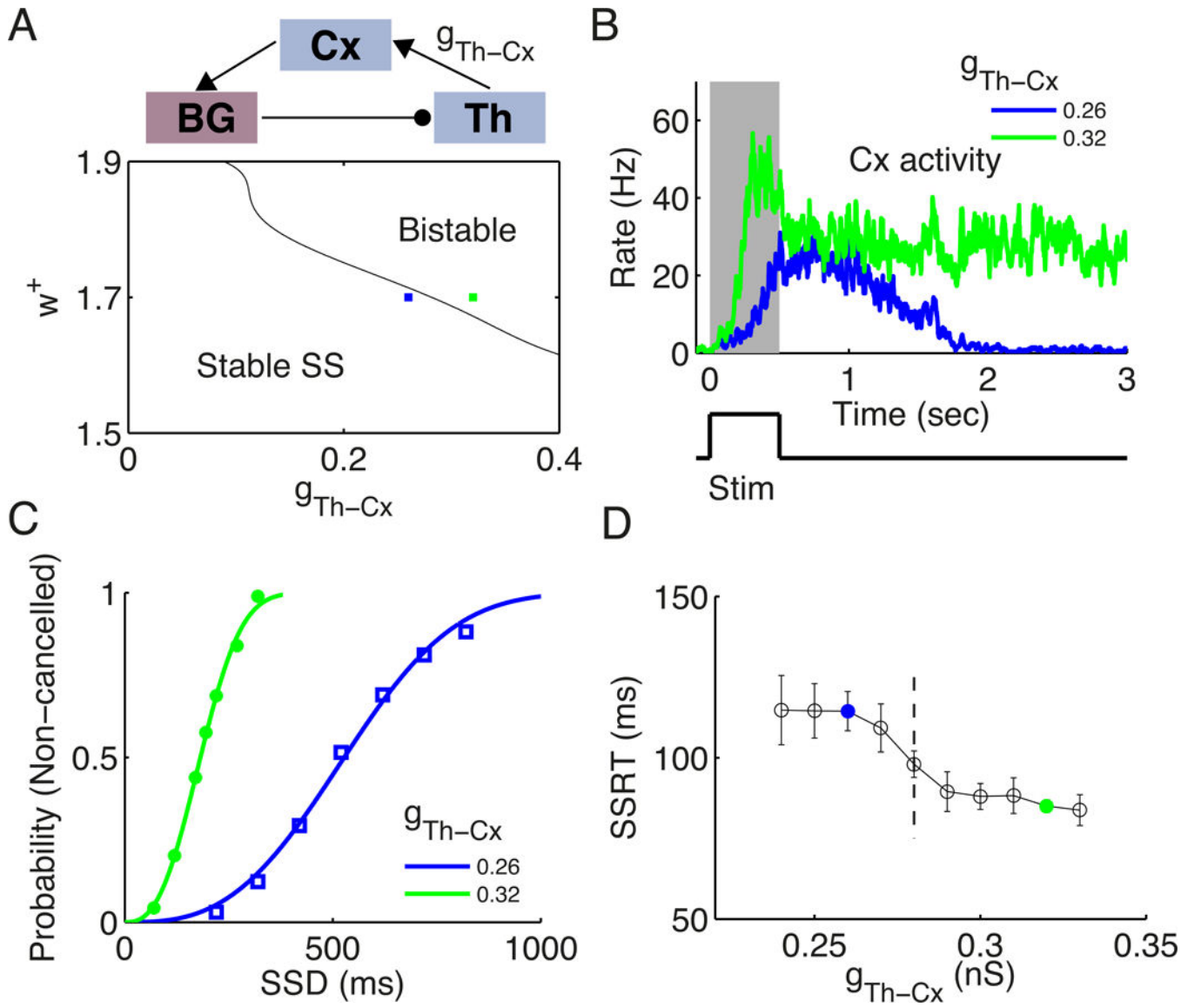

Figure 5. Inhibitory control measured by SSRT is enhanced by stronger reverberatory dynamics

(A) Upper panel: schematic of the Cx-BG-Th loop. Lower panel: The state diagram as a function of the local recurrent feedback strength w^+ in the Cx and the subcortico-cortical loop feedback strength g_{Th-Cx}. Stable SS: region where only the spontaneous state (SS) is stable. Bistable: region where both the SS and target-selective elevated persistent activity state are stable. Two sample networks are indicated in the state diagram at g_{Th-Cx} = 0.26 nS (blue) and 0.32 nS (green) with w^+ = 1.7. (B) Neuronal activity of the winner population in the Cx in response to a brief stimulus. The green and blue curves correspond to the green and blue squares in (A). The gray-shaded area shows the neuronal activities during stimulus onset, which lasts for 0.5 sec (lower panel). (C) Inhibition functions for g_{Th-Cx} = 0.26 nS and 0.32 nS, respectively. (D) Two-level modulation of the SSRT when increasing g_{Th-Cx} gradually from a regime not supporting persistent activity to a regime supporting persistent activity with a fixed w^+ (w^+ = 1.7). The colored points correspond to those in (A). The vertical dashed line indicates the value of g_{Th-Cx} when crossing the boundary for the two

regimes. Error bars indicate s.d. of SSRT values estimated for different SSD. The inhibition functions in (C) are fitted by the Weibull function.

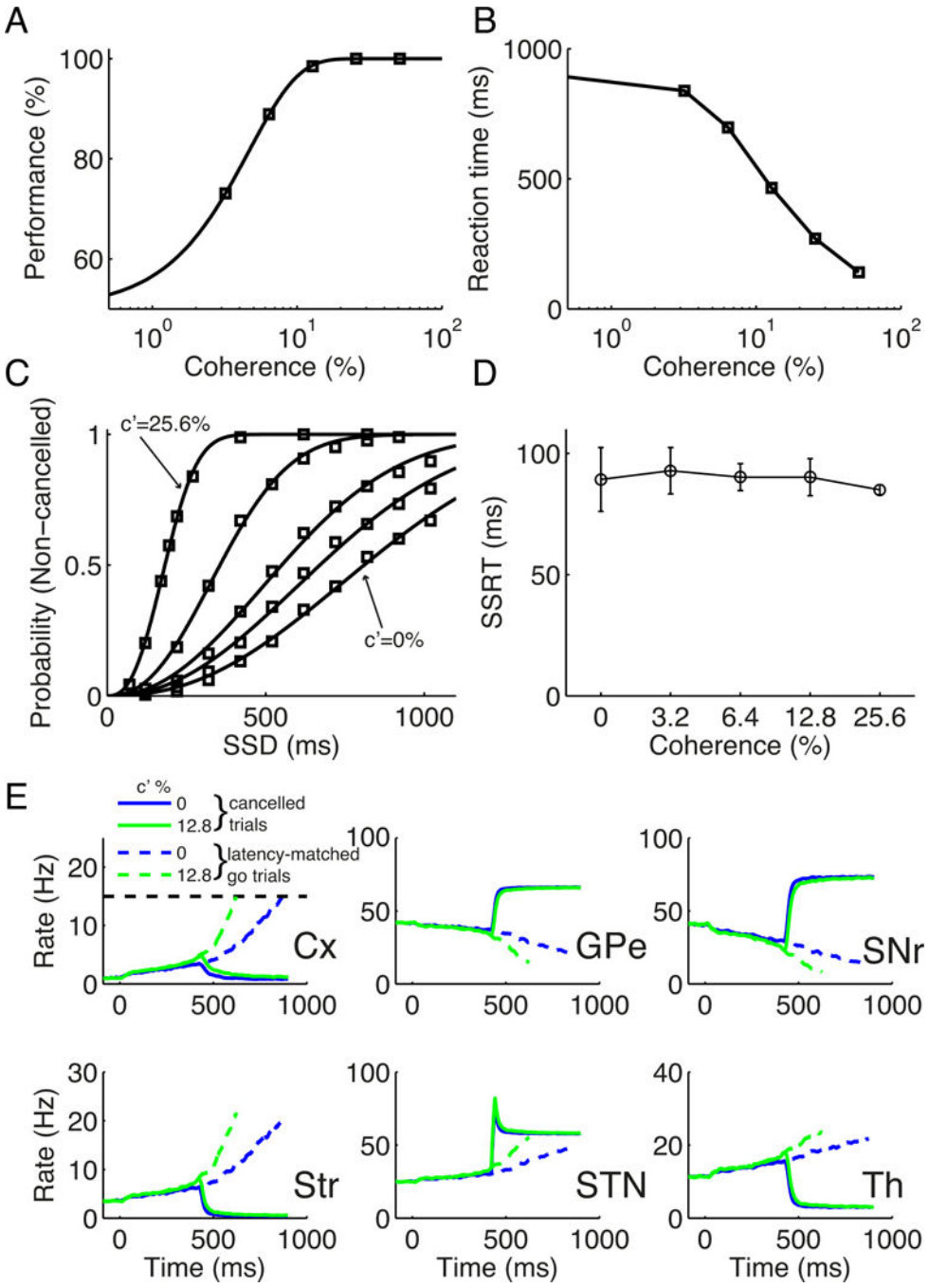

Figure 6. SSRT is independent of task difficulty in perceptual decision making

(A–B) Performances (A) and mean RTs (B) from model simulation of a random-dot motion direction discrimination task with a stop signal. (C) Inhibition functions for different task difficulty represented by motion coherence of the random-dot input, c'. The values of c' from bottom to top are 0%, 3.2%, 6.4%, 12.8% and 25.6%, respectively. The inhibition functions are fitted by the Weibull function. (D) The SSRT as a function of c', showing no statistically significant dependence. Error bars indicate s.d. of SSRT values estimated for those SSDs with corresponding non-cancelled probability within the interval (0.1, 0.9). (E)

Mean neuronal activities for successful stop signal trials (solid curves) and latency-matched go trials (dashed curves) with SSD = 420 ms when $c' = 0\%$ (blue) and 12.8% (green). The mean activities are obtained from averaging over 200 trials of the same type.

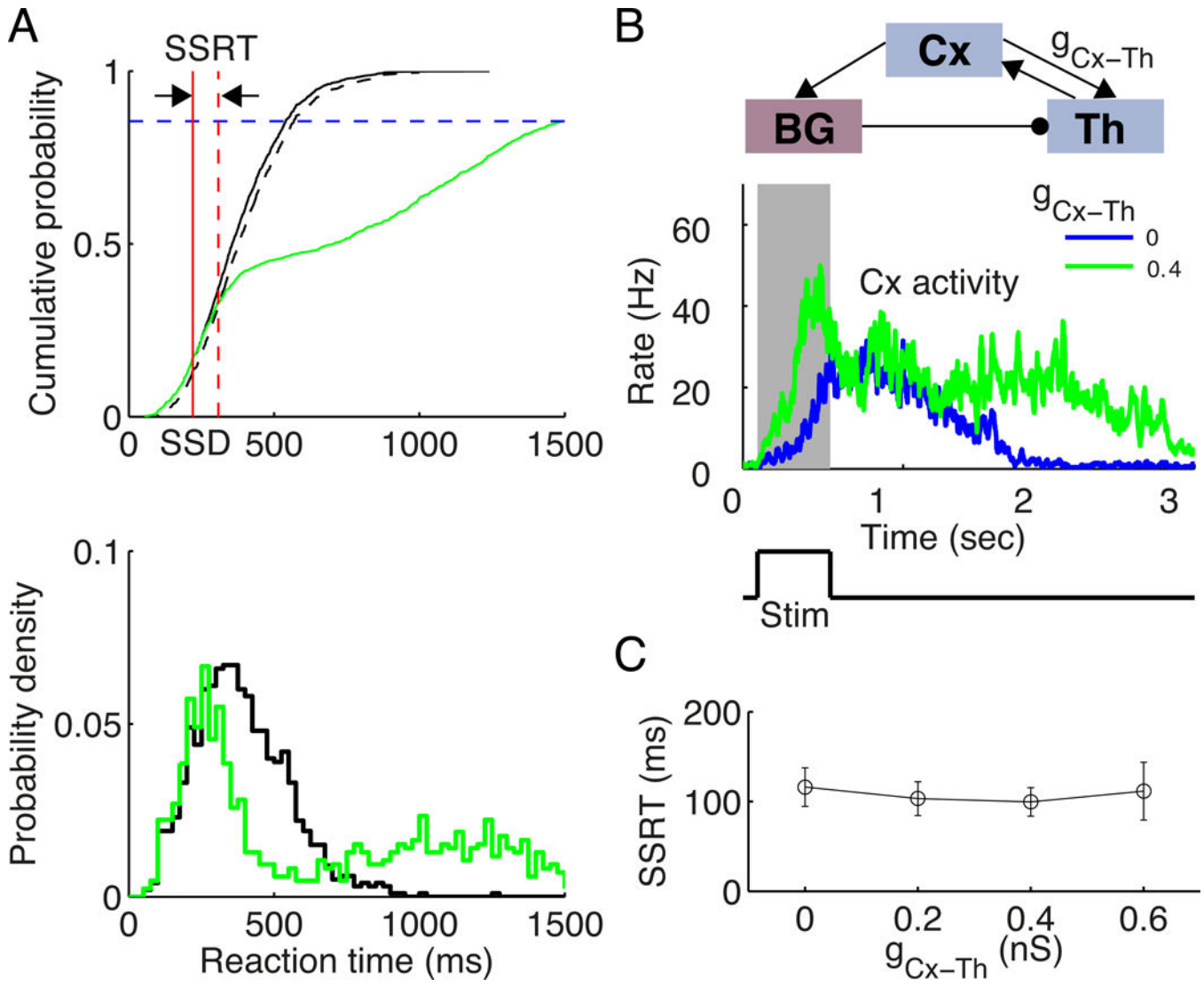

Figure 7. Impact of Cx-Th sub-loop on inhibitory control

(A) Lower panel: the RTs of go trials (black) and non-cancelled stop signal trials (green). Note the double peaks in the distribution of the non-cancelled stop signal trials. Here the corticothalamic connection strength g_{Cx-Th} = 0.4 nS. Upper panel: modified integration method for estimating SSRT, illustrated with SSD = 220 ms. Black curve represents the cdf for RTs of the go trials, and green curve represents the cdf for the non-cancelled trials, scaled by the non-cancelled probability (blue dashed line). The dashed black curve represents the 99.9% confidence interval (CI) of the cdf for RTs of go trials. The vertical red dashed line represents the intersection time of the green curve with the black dashed curve. The red solid line indicates the SSD. The interval between the vertical solid and dashed red lines gives the SSRT. (D) Upper panel: schematic of the circuit. Middle panel: neuronal activities of the winner population in the Cx in response to a brief stimulus for g_{Cx-Th} = 0 (blue) and 0.4 nS (green), respectively. The gray-shaded area indicates neuronal activities during stimulus onset, which lasts for 0.5 sec (lower panel). The stimulus is a random-dot

with $c' = 25.6\%$. (E) SSRT is insensitive to g_{Cx-Th}. Error bars indicate s.d. of SSRT values estimated for different SSDs. In this figure $g_{Th-Cx} = 0.26$ nS.

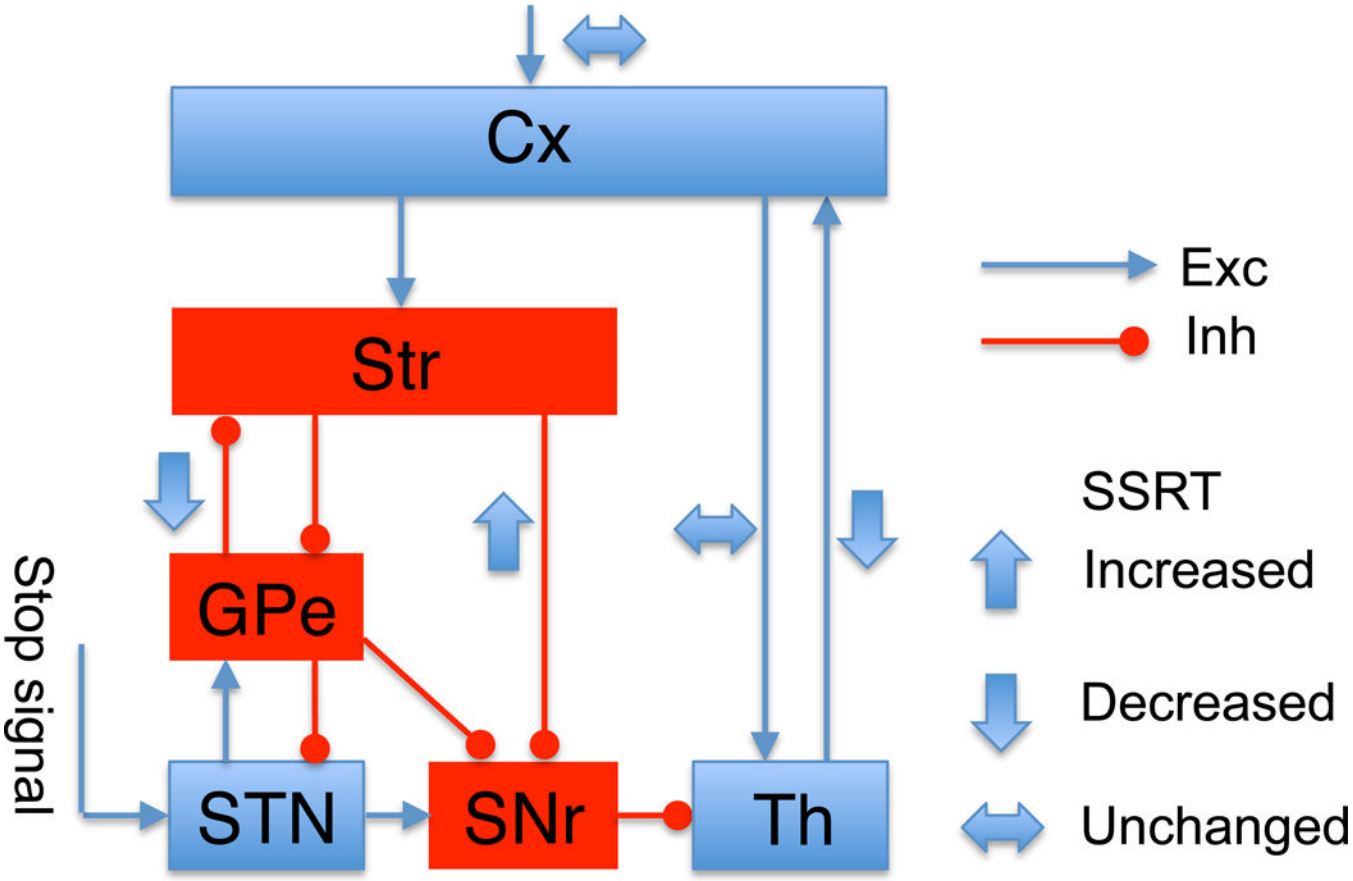

Figure 8. Summary of the dependence of SSRT on various inter-area connections or the external stimulus

The SSRT may be increased (wide up arrows), decreased (wide down arrows), or unchanged (wide horizontal arrows) by an increase of the connection strength from one area to another area, or of the task difficulty reflected in the input to the Cx. Other conventions are the same as in Figure 1.